



**HAL**  
open science

## Hydraulic fracture simulation using the GEOS code

Murad S. Abuaisha, David Eaton, Jeffrey Priest, Ron Wong

► **To cite this version:**

Murad S. Abuaisha, David Eaton, Jeffrey Priest, Ron Wong. Hydraulic fracture simulation using the GEOS code. Microseismic Industry Consortium: Annual Research Report, Volume 5, 2015. hal-02461042

**HAL Id: hal-02461042**

**<https://minesparis-psl.hal.science/hal-02461042>**

Submitted on 3 Feb 2020

**HAL** is a multi-disciplinary open access archive for the deposit and dissemination of scientific research documents, whether they are published or not. The documents may come from teaching and research institutions in France or abroad, or from public or private research centers.

L'archive ouverte pluridisciplinaire **HAL**, est destinée au dépôt et à la diffusion de documents scientifiques de niveau recherche, publiés ou non, émanant des établissements d'enseignement et de recherche français ou étrangers, des laboratoires publics ou privés.

## Chapter 8

# Hydraulic fracture simulation using the GEOS code

*Murad AbuAisha<sup>a,b</sup>, David W. Eaton<sup>a</sup>, Jeffrey Priest<sup>b</sup> and Ron Wong<sup>b</sup>*

<sup>a</sup> Dept. of Geoscience, Univ. of Calgary, Calgary, AB, T2N 1N4, Canada.

<sup>b</sup> Dept. of Civil Engineering, Univ. of Calgary, Calgary, AB, T2N 1N4, Canada.

E: murad.abuaisha@ucalgary.ca

### Summary

This paper discusses the issues involved in the development of a fully three-dimensional, massively parallel, finite element based simulation framework (GEOS) for addressing the fully coupled, hydro-mechanical behavior of jointed and fractured unconventional reservoirs to hydraulic stimulation. The framework is capable of describing the problems on large scale by implementing models for multi-scale treatment of geomaterials. Besides, the framework is able to explicitly representing fracture nucleation and propagation by using the technique of evolving mesh topology for both the fluid and solid meshes. It is also worthwhile to mention that the GEOS framework is designed to combine continuum and discontinuum approaches.

### 8.1 Introduction

Hydraulic fracturing consists of injecting a viscous fluid into a well under high pressure to initiate and propagate a fracture. The design of a treatment relies on the ability to predict the opening and the size of the fracture as well as the pressure of the fracturing fluid, as a function of the properties of the rock and the fluid. In that respect, the availability of numerical approaches to solve hydraulic stimulation problems is especially valuable. The construction of such approaches is the topic of this paper.

The paper describes verification of a fully three-dimensional, massively parallel, finite element based simulation framework (GEOS) for addressing the fully coupled, hydro-mechanical behavior of jointed and fractured unconventional

reservoirs to hydraulic stimulation. Unlike many common engineering tools to describe hydraulic stimulation the GEOS has the following characteristics:

- the framework is appropriate to a wide range of problems. It does not rely on simplifying assumptions concerning fracture geometry, density or material behavior;
- the massively parallel nature of the calculations allows the code to address problems up to reservoir scale on large-scale computer clusters;
- the general nature of the framework allows it to provide a way of not only capturing more of the detail of the physical problem, but can also be used to assess the sensitivity of other tools to the assumptions of their methods, including the role of material properties, fracture mechanics models, fluid properties, and the presence and representation of pre-existing and induced fractures.

The first objective of the paper is to describe the framework of GEOS. The second objective seeks to demonstrate the code's numerical implementation by comparing with known analytical solution of Savitski and Detournay (2002) for both viscosity and toughness dominated radial fracture propagation.

### 8.2 Methodology of the GEOS code

Realistic simulations of hydraulic fracturing require that several phenomena to be taken into consideration. Such phenomena in-

clude:

1. fracture interaction in the presence of three-dimensional heterogeneous properties;
2. providing competing paths for the flow paths;
3. the effect of the change of stress field, resulting from the development of fluid pressure field, on fracture propagation and on the stress state of far field heterogeneities/fractures;
4. multi-scale treatment of geomaterials – dual scale paradigm;
5. explicit representation of fracture nucleation and propagation, and;
6. representation of damage.

To account for such phenomena, the GEOS code provides a fully coupled system consisting of the standard equations of motion to model the rock matrix, and a parallel plate flow simplification (i.e. lubrication theory) to model the flow in the fracture. The evolution of a fracture proceeds along element interfaces, and fluid elements are inserted at the newly formed crack faces. Thus, as the fracture grows, the mesh topology for both the fluid and solid meshes evolves.

### 8.2.1 Finite element: Solid mechanics

To provide a mean to couple changes in fluid pressure in a given crack with the stress state throughout the problem domain, the FEM is applied to the equation of motion. The application of the FEM to the equation of motion on a solid body  $\Omega$ , with  $\Gamma_t$  being the boundary where external tractions are applied, and  $\Gamma_c$  the boundary where crack exists, gives,

$$\nabla_j \sigma_{ij} + p_f n_i + \rho_s b_i = \rho v_i, \quad (8.1)$$

$$\begin{aligned} & \int_{\Gamma_t} \Phi_a t_i dA - \int_{\Omega} \frac{\partial \Phi_a}{\partial x_j} \sigma_{ij} dV + \int_{\Gamma_c} \Phi_a p_f n_i dA \\ & + \int_{\Omega} \Phi_a \rho_s (b_i - v_i) dV = 0, \end{aligned} \quad (8.2)$$

with  $\Phi_a$  are the shape functions at node  $a$ ,  $t_i = \sigma_{ij} n_j$  is the surface traction on the boundary  $\Gamma_t$ ,  $\sigma_{ij}$  is the Cauchy stress tensor,  $\mathbf{n}$  is the outward normal vector,  $p_f$  is the fluid pressure inside the fracture<sup>1</sup>,  $\rho_s$  is the solid density,  $b_i$  is the body force per unit mass, and  $v_i$  is the acceleration. The same shape functions are used to interpolate the primary unknowns of displacement field  $u_i$  and the pore fluid pressure  $p_f$ . The approach is the conventional Galerkin of the FEM.

<sup>1</sup>It is conceivable, from eq. (8.1), that the pressure gradients due to fluid diffusion in the rock matrix/outside the fractures are neglected.

<sup>2</sup>A fracturing criterion may not be needed if the fracturing regime is viscosity dominated; this will be discussed later in this paper.

### 8.2.2 Finite volume: Fluid mechanics

To model the flow in the fractures, the parallel plate flow (lubrication theory) is used. The parallel plate solution for the Navier–Stokes equation leads to the commonly used “cubic law”. The flow  $q$  between two parallel plates with apertures  $w$  and pressure difference  $\Delta p$  is given by,

$$q = \frac{w^3}{12\mu} \Delta p, \quad \text{assuming 1-dimensional flow} \quad (8.3)$$

with  $\mu$  being the dynamic viscosity of the fluid.

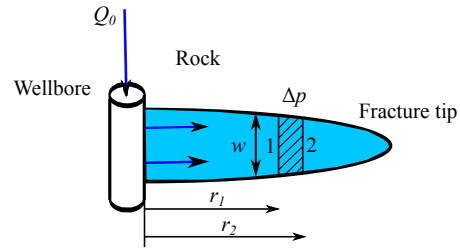


Figure 1: Flow in the fractures, the parallel plate flow (lubrication theory).

The non-linear differential equation for the aperture profile of a radial fracture can be derived from the lubrication theory,

$$\frac{\partial w}{\partial t} = \frac{1}{12\mu} \frac{1}{r} \frac{\partial}{\partial r} \left( r w^3 \frac{\partial p}{\partial r} \right). \quad (8.4)$$

Following eq. (8.3) and eq. (8.4), the rate of mass flow  $m_{12}$  from an edge 1 to a face 2 is expressed as,

$$\frac{dm_{12}}{dt} = \frac{w^3 r_2}{12\mu r_1} \rho_f (p_2 - p_1). \quad (8.5)$$

where  $\rho_f$  is the fluid density,  $r_1$  is the length of the edge over which the flow is taking place, and  $r_2$  is the distance from the edge to the face center, see Fig. (1).

### 8.2.3 Fracturing criterion

A rupture criterion<sup>2</sup> is first specified and evaluated on every internal face. Upon completion of a closed path of surfaces where either the rupture criterion is satisfied, or the surface is external to the body, a new set of nodes, edges, and faces are generated, and the mesh topology is updated. To account for geologic materials high non-linearities, the stress intensity factor is calculated at the crack tip for Mode I and Mode II of fracture propagation. The energy release rate is estimated by multiplying the field of displacement by the nodal forces at the crack tip. The energy release rate is then converted to the stress intensity factor.

## 8.2.4 Fracturing failure mechanisms in GEOS

For the case of a propagating fracture due to hydraulic fracture stimulation, micro-seismic data collected from a number of projects indicate bulk fracture propagation of  $O(10^1)$  m/s  $\ll O(10^3)$  for the Rayleigh wave speed in most geologic materials. This is counterintuitive when considering fracture mechanics, where fractures in tension (Mode I) generally propagate near the Rayleigh wave speed. This remains true at the microscale; however, fracture propagation is constantly mediated by fluid forcing, which is dependent on maintaining a pressure front near the tip of the fracture.

The time constant associated with this pressure front development is much larger than that associated with the Rayleigh wave speed. If we resort to theoretical consideration of fluid-driven fractures in an elastic medium, the anecdotally observed propagation velocity is recovered, Johnson et al. (2013),

$$\bar{v}_p = 4\mu K_f^2 v_f \sigma_0^{-3}, \quad (8.6)$$

where  $\mu$  is the viscosity,  $v_f$  is the mean fluid velocity into the fracture,  $K_f$  is the bulk modulus of the fluid, and  $\sigma_0$  is the confining pressure. For typical rock properties at confining pressures of 10–100 MPa, the tip velocity is  $O(1 - 10)$  m/s.

In general, this suggests stress equilibrium in the far field for bulk fracture propagation<sup>3</sup>, such that there exists a temporal scale separation between the resolution of stress in the local region of a fracture and that at larger scales. This region, referred to in the literature as the “process zone”, can often be decoupled from the solution of the mechanics in the rest of the domain (referred to as the “far field”).

Failure, however, in a realistic geological material can be much more complex than the isotropic, homogeneous, elasto-brittle materials classically addressed in the linear elastic fracture mechanics (LEFM) literature, especially given the bedded, anisotropic, and discontinuous nature of geologic material. When focusing only on the mechanisms involved at the process zone of a propagating hydraulic fracture, the complexities of crack coalescence, fluid interaction, complex stress field anisotropy, and grain boundary effects can be readily seen, but complexities exist across length scales. Careful field studies and analyses have, for instance, observed that discontinuities exhibit a smooth length scale distribution across scales from millimeters to kilometers and are widely believed to be due to growth processes that do not have characteristic length scales, Johnson et al. (2013).

In this study, the developers of the GEOS focus on how to resolve this problematic situation via a sequential, hierarchical multiscale method, which, at its base, relies on a dual-scale representation of inhomogeneity and damage. By overlapping the spatial scales at which successively coarser simulations are performed, effective upscaling can be managed and

scale-dependent relations with appropriate contributions from finer scales can be developed. For failures along pre-existing surfaces, the developers use a numerical framework amended to accommodate arbitrarily large strains through an advection-free scheme; the amendments are described next for completeness, (Johnson et al. (2013); Settgest et al. (2004)).

## 8.2.5 Failure along interfaces: Large strains in the FEM

For the case of failures either along the developed fracture network or in regions where the stress field has been rotated enough to affect failure in pre-existing fractures, the failures are often Mode II (strike-slip) events, as they are predominantly for laboratory hydraulic fracture experiments.

One problem that has yet to be addressed is the ability to capture arbitrarily large shear strains at the interfaces of moving joints in a tractable numerical framework, where the behavior at the interface is represented by phenomenological joint models. Johnson et al. (2013) have addressed an improved approach of the advection-free scheme based on the common plane method often used in the DEM. In this approach the elements are brought into contact normally, then sheared while conserving energy. The algorithm also assures linear and angular momentum conservation by evaluating the shape function derivatives of the finite elements on the external faces and applying the resultant forces from the phenomenological joint models to the nodes, accordingly. The result of this procedure is an advection-free method of representing large strains across interfaces.

## 8.2.6 Multi-scale treatment of geomaterials

Geomaterials exhibit two main attributes that make them natural candidates for a multi-scale treatment: 1- the phenomenology of interest possesses no similarity relations across scales and, 2- the size distribution of discontinuities is smooth across several orders of magnitude, making it impossible to rigorously define a Representative Elementary Volume (REV) for the general case (though, specific systems may exhibit natural scale decoupling). The former means that models will likely need to be scale-dependent, while the latter means that material behavior cannot be characterized locally and, therefore, effective continuum representations will always have some error associated with the locality assumption. The situation is not hopeless: there are many field cases where the assumptions of an effective continuum do hold or at least do not introduce significant error; analysts can often identify natural scale decoupling due to the specific geology (e.g., local features limit the size distribution of the discontinuities), or the phenomenology of interest is not affected by the discontinuities (e.g., long period wave propaga-

<sup>3</sup>Since at far field  $v_f \rightarrow 0$  and  $\sigma_0$  is no longer a function of the propagation velocity.

tion). Here, the authors are concerned with the cases where the system does not permit such simplifications which requires consideration of many scales.

### 8.2.6.1 *The dual scale paradigm*

An approach to multi-scale modeling is developed through the assumption that for any arbitrary length scale, discontinuities can be represented at two scales: 1- either the response of each discontinuity is represented directly (explicitly) and material response is defined through the aggregate of individual discontinuities (i.e., discontinuous modeling); or 2- through homogenization of the behavior of a REV of such features (i.e., effective continuum). The approach in GEOS seeks to represent both scales at any particular arbitrary length scale, where discontinuities near the length scale of interest are represented explicitly while features smaller than a threshold are represented via an effective continuum, where the constitutive model used is necessarily scale-dependent and derived from finer scale simulations when the scale of the REV is above the percolation limit.

### 8.2.6.2 *Fracture nucleation and propagation*

Linear Elastic Fracture Mechanics (LEFM) allows the prediction of the propagation of a single, flat crack (or fracture) embedded in a homogeneous, isotropic, elastic solid body. The analytical solutions are derived from Griffith theory and can be obtained by computing Stress Intensity Factors (SIFs) in modes I, II and III. As a consequence, most of the existing models of hydraulic fracturing consider the rock mass as an elastic, impermeable solid. This approach is suitable to distinguish between toughness-dominated and viscosity-dominated fracture propagation regimes. Yet, it is constrained by restrictive assumptions and does not allow coupling fracture propagation to the fabric changes undergone by the rock mass. Besides, neglecting micro-cracking ahead of the fracture tip leads to over-estimated fracture front velocity. Moreover, according to the theory of elasticity, the presence of cracks around the fracture tip induces stress perturbations, and thus impact SIFs. Some work has been proposed to address this issue. However, this remains an open research issue for fully three-dimensional solids.

One method of capturing the damage zone in finite element models of hydraulic fracturing is to define an inelastic zone where plastic deformation localizes. The numerical solution is highly mesh-dependent, however, the localized zone narrows with mesh-refinement.

The GEOS approach overcomes all the aforementioned obstacles by the techniques of remeshing and the dual scale paradigm to account for heterogeneities.

<sup>4</sup>This could be related to the approaches the developers are adopting to ensure small strains and hence applying the laws of energy and momentum conservation.

<sup>5</sup>Fully implicit time integration schemes are deemed appropriate for hydraulic fracture simulations due the large time scales associated with such simulations.

### 8.2.6.3 *Effective continuum representation: Representation of damage*

There are a number of approaches to represent the effective hydrological and mechanical response of geomaterials to progressive damage. These can be categorized into micro-scale derived models, purely phenomenological models, micro-scale enriched methods (with varying levels of fidelity), and hybrids of the aforementioned. There are also special considerations for calculating the effects on permeability through the use of homogenization techniques.

Here, the developers of GEOS are using a hybrid model of damage nucleation and accumulation at the effective continuum scale, where the micro-scale degrees-of-freedom are explicitly captured using finite, rectilinear failure surfaces. The developers are currently using small damage assumptions, as well, where micro-scale damage does not evolve mechanical changes at the macro-scale. This is a strong assumption that will be remediated in further work<sup>4</sup>.

### 8.2.7 Time marching scheme

Though not totally appropriate<sup>5</sup>, an explicit method is chosen to run the time integration scheme. A standard Newmark method is applied to the finite element equations in (8.1) and (8.2), while a standard forward Euler method is applied to the finite volume equation in (8.3), Settgest et al. (2004).

## 8.3 Propagation of a penny-shaped fluid-driven fracture

In order to understand the mechanism of fluid-driven fracturing as well as to validate the GEOS code, this paper presents an analysis of the propagation of a penny-shaped hydraulic fracture in an impermeable elastic rock. The fracture is driven by an incompressible Newtonian fluid injected from a source at the center of the fracture. The fluid flow is modeled according to lubrication theory, while the elastic response is governed by a singular integral equation relating the crack opening and the fluid pressure. It is shown that the scaled equations contain only one parameter, a dimensionless toughness, which controls the regimes of fracture propagation. Asymptotic solutions for zero and large dimensionless toughness are constructed.

The first objective of this section is to construct rigorous solutions for the problem of a penny-shaped fluid-driven fracture, with a clear statement of their range of applicability. The other objective arises from a long-standing debate on the relevance of the rock toughness. This question is of fundamental importance

for numerical modeling. If toughness is relevant, the shape of the fracture must be determined by tracking the fracture tip; if not, the fracture shape can be identified by the fluid front, which is much easier to follow than the fracture edge.

An entirely different approach to the issue of toughness invokes an argument based on the ratio of the energy dissipated in the rock to create new fracture surfaces to the energy dissipated in the fluid by viscous flow. According to this argument, the influence of toughness can be neglected if this energy ratio is small. For a hydraulic fracture in plane strain, this criterion yields a critical value for a dimensionless toughness below which toughness is negligible. Interestingly, this criterion does not depend on the confining stress<sup>6</sup>. The energy argument suggests that there must be three regimes of the propagation: viscosity-dominated (in which the toughness may be neglected), toughness-dominated (in which the viscosity may be neglected), and transient (in which both parameters are important), see Savitski and Detournay (2002).

### 8.3.1 Problem formulation

Consider an axisymmetric hydraulic fracture propagating in an infinite impermeable elastic medium characterized by Young's modulus  $E$ , Poisson's ratio  $\nu$ , and toughness  $K_{Ic}$  (Fig. 2). An incompressible Newtonian fluid with viscosity  $\mu$  is injected at the center of the fracture at constant volumetric rate  $Q_0$ . We seek to determine the crack aperture  $w(r, t)$  as a function of the radial coordinate  $r$  and time  $t$ , the net pressure  $p(r, t)$  (the difference between the fluid pressure  $p_f$  and the far-field compressive stress  $\sigma_0$  perpendicular to the fracture plane), and the fracture radius  $R(t)$ .

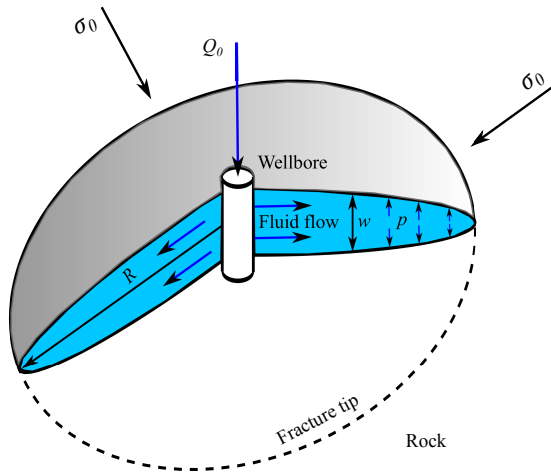


Figure 2: A penny-shaped hydraulic fracture: radial propagation, modified after Savitski and Detournay (2002).

<sup>6</sup>This conclusion will be discussed later in this paper.

<sup>7</sup>The assumption that the fluid front coincides with the crack tip results in a pressure singularity at the tip.

<sup>8</sup>See Savitski and Detournay (2002) for details.

<sup>9</sup>The equation is written in a Fourier's transform.

Several assumptions are introduced to simplify this problem:

1. the fluid is injected from a point source (i.e. the wellbore radius is negligible compared to the fracture radius);
2. the fluid reaches the tip of the crack (i.e. the lag between the fracture tip and the fluid front is very small compared to the fracture radius)<sup>7</sup>; and,
3. the fracture propagates continuously in mobile equilibrium;
4. lubrication theory is applicable.

The legitimacy of Assumption 2 is based on an analysis of the near tip region of a fluid-driven fracture<sup>8</sup>, which indicates that the lag  $\lambda$  reaches a maximum value  $\lambda_0 \sim \mu \bar{v}_p E^2 \sigma_0^{-3}$  with  $\bar{v}_p$  denoting the tip velocity when  $K_{Ic} = 0$ . For typical values of the parameters,  $\lambda_0$  is of the order of  $10^{-1}$  m and thus generally very small compared to the fracture radius, which can reach dimension of order of  $10^2$  m. Furthermore, the actual lag  $\lambda$  could be very small compared to  $\lambda_0$ , if  $K_{Ic} > 0$ . By neglecting the lag, the solution does not depend on the far-field stress  $\sigma_0$ , which enters the formulation only as a reference stress.

The complete formulation of this problem relies on equations from elasticity and lubrication theory, on a fracture propagation criterion from linear elastic fracture mechanics, and on boundary conditions at the inlet and at the tip of the fracture. The two coupled equations involving the fracture opening  $w(r, t)$  and net pressure  $p(r, t)$  consist of a non-local integral relation from elasticity<sup>9</sup>, by Atkinson (1991),

$$w = \frac{8R}{\pi E'} \int_{r/R}^1 \frac{\xi}{\sqrt{\xi^2 - (r/R)^2}} \int_0^1 \frac{x p(x\xi R, t)}{\sqrt{1 - x^2}} dx d\xi, \quad (8.7)$$

and a non-linear differential equation from lubrication theory, by Lamb (1945),

$$\frac{\partial w}{\partial t} = \frac{1}{12\mu} \frac{1}{r} \frac{\partial}{\partial r} \left( r w^3 \frac{\partial p}{\partial r} \right). \quad (8.8)$$

In the above,  $E'$  is the plane strain modulus, which can be expressed in terms of  $E$  and  $\nu$  as  $E' = E/(1 - \nu^2)$ . According to linear elastic fracture mechanics, the fracture propagation criterion takes the form,

$$K_I = K_{Ic}, \quad (8.9)$$

where  $K_I$  denotes the mode I stress intensity factor and  $K_{Ic}$  the material toughness. For a penny-shaped crack,  $K_I$  can be expressed as in Atkinson (1991),

$$K_I = \frac{2}{\sqrt{\pi r}} \int_0^R \frac{p(r, t)}{\sqrt{R^2 - r^2}} r dr. \quad (8.10)$$

The fracture tip is characterized by zero fracture opening,

$$w = 0, \quad r = R, \quad (8.11)$$

and a no-flow condition  $q = 0$ , which can be expressed in terms of opening and pressure by means of Poiseuille law,

$$q = 0 = -\frac{w^3}{12\mu} \frac{\partial p}{\partial r} \implies w^3 \frac{\partial p}{\partial r} = 0, \quad r = R. \quad (8.12)$$

Injection of fluid from the borehole is idealized by a source at the center of the fracture. Based on mass balance considerations, the source condition can be expressed as,

$$2\pi \lim_{r \rightarrow 0} rq = Q_0, \quad (8.13)$$

It follows from (8.13) that  $q \sim 1/r$  near the source. According to Poiseuille law (8.12), the fluid pressure is thus logarithmically singular at the source,  $p \sim -\ln r$ . The source can alternatively be taken into account by the global mass balance,

$$Q_0 t = 2\pi \int_0^R wr \, dr. \quad (8.14)$$

The set consisting of the elasticity eq. (8.7), Reynolds equation (8.8), the propagation criterion (8.9), the inlet condition (8.13) or (8.14) and the tip conditions (8.11) or (8.12) forms a complete system for determining  $w(r, t)$ ,  $p(r, t)$ , and  $R(t)$  with  $0 \leq r \leq R(t)$ ,  $t \geq t_0$ .

### 8.3.2 Analytical solution

The objective of this part is to find an analytical solution for the problem defined previously. The analytical solution is to be employed to understand the mechanism of fluid-driven fracturing which is of enormous importance to our research. To get the solution, first it is convenient to define a viscosity  $\mu'$  and a toughness  $K'$ , respectively proportional to  $\mu$  and  $K_{Ic}$ , to avoid carrying numerical factors in the equations,

$$\mu' = 12\mu, \quad K' = 4 \left( \frac{2}{\pi} \right)^2 K_{Ic}. \quad (8.15)$$

It is also natural to introduce the dimensionless toughness  $\mathcal{K}$  as expressed in Savitski and Detournay (2002),

$$\mathcal{K} = K' \left( \frac{t^2}{\mu'^5 Q_0^3 E'^{13}} \right)^{1/18}, \quad (8.16)$$

a dimensionless viscosity  $\mathcal{M}$  is logically defined as in Savitski and Detournay (2002) as well,

$$\mathcal{M} = \mu' \left( \frac{Q_0^3 E'^{13}}{K'^{18} t^2} \right)^{1/5}, \quad (8.17)$$

the dimensionless viscosity  $\mathcal{M}$  and toughness  $\mathcal{K}$  are simply related by,

$$\mathcal{M} = \mathcal{K}^{-18/5}. \quad (8.18)$$

The analytical solution, in a toughness scaling, is obtained by scaling the set of equations and boundaries described previously. Scaling of the problem hinges in defining dimensionless crack opening  $\Omega$ , net pressure  $\Pi$  and fracture radius  $\gamma$ , see Savitski and Detournay (2002) for details,

$$\begin{aligned} w(r, t) &= \epsilon(t) L(t) \Omega(\rho, \tilde{h}(t)); \\ p(r, t) &= \epsilon(t) E' \Pi(\rho, \tilde{h}(t)); \\ R(r, t) &= L(t) \gamma(\tilde{h}(t)), \end{aligned} \quad (8.19)$$

in which,  $\rho = r/R(t)$  ( $0 \leq \rho \leq 1$ ) is the dimensionless coordinate,  $\epsilon(t)$  is a small number,  $L(t)$  is a length scale of the same order of magnitude as the fracture radius  $R(t)$ , and  $\tilde{h}(t)$  is a dimensionless parameter that depends monotonically on time  $t$ .

we now seek a solution of the form  $\mathcal{F} = \{\Omega, \Pi, \gamma\}$  to order of  $\mathcal{M}$  in the form of regular asymptotic expansion,

$$\mathcal{F}(\mathcal{M}) = \mathcal{F}_0 + \mathcal{M}\mathcal{F}_1 + O(\mathcal{M}^2), \quad (8.20)$$

where  $\mathcal{F}_0 = \{\Omega_0, \Pi_0, \gamma_0\}$  and  $\mathcal{F}_1 = \{\Omega_1, \Pi_1, \gamma_1\}$ . The following sets of equations for the zero- and first-order terms are obtained:

- the zero-order solution,  $\mathcal{F}_0$ , corresponds to an inviscid fluid ( $\mathcal{M} = 0$ ) and is given in a closed form by Savitski and Detournay (2002),

$$\begin{aligned} \Pi_0 &= \frac{\pi}{8} \left( \frac{\pi}{12} \right)^{1/5} \approx 0.3004; \\ \Omega_0 &= \left( \frac{3}{8\pi} \right)^{1/5} (1 - \rho^2)^{1/2}; \\ \gamma_0 &= \left( \frac{3}{\pi\sqrt{2}} \right)^{2/5} \approx 0.8546, \end{aligned} \quad (8.21)$$

- the first-order,  $\mathcal{F}_1$ , solution can also be expressed as in Savitski and Detournay (2002),

$$\begin{aligned} \Pi_1 &= \Pi_1^* - A \left[ \frac{1}{3} \ln \rho - \frac{1}{5} \ln(1 - \rho^2) \right]; \\ \Omega_1 &= B(1 - \rho^2)^{1/2} - \frac{8}{3\pi} A \gamma_0 \left[ \left( \ln 2 - \frac{4}{5} \right) \times \right. \\ &\quad \left. (1 - \rho^2)^{1/2} + \rho \cos^{-1} \rho - \frac{6}{5} I^*(\rho) \right]; \\ \gamma_1 &= -\frac{544}{75\pi^2} \approx -0.7349, \end{aligned} \quad (8.22)$$

where the constants  $\Pi_1^* \approx 0.6380$ ,  $A \approx 1.709$ , and  $B \approx 0.8264$ . The function,  $I^*(\rho)$ , defined as,

$$I^*(\rho) = \int_{\rho}^1 \sqrt{\frac{1 - \xi^2}{\xi^2 - \rho^2}} \cos^{-1} \xi \, d\xi \quad (8.23)$$

has to be evaluated numerically.

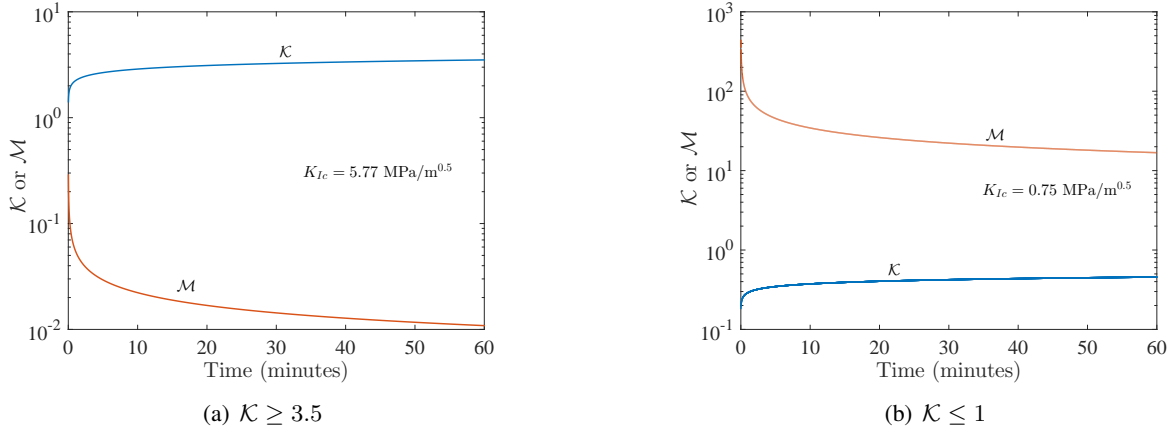


Figure 3: The development of the dimensionless toughness and viscosity over an hour injection test according to the rock properties and operating conditions described in Johnson et al. (2013): a) toughness dominated fracturing  $\mathcal{K} \geq 3.5$ , b) viscosity dominated fracturing  $\mathcal{K} \leq 1$ . The regimes of fracture propagation will be further discussed in Sect. (8.3.4)

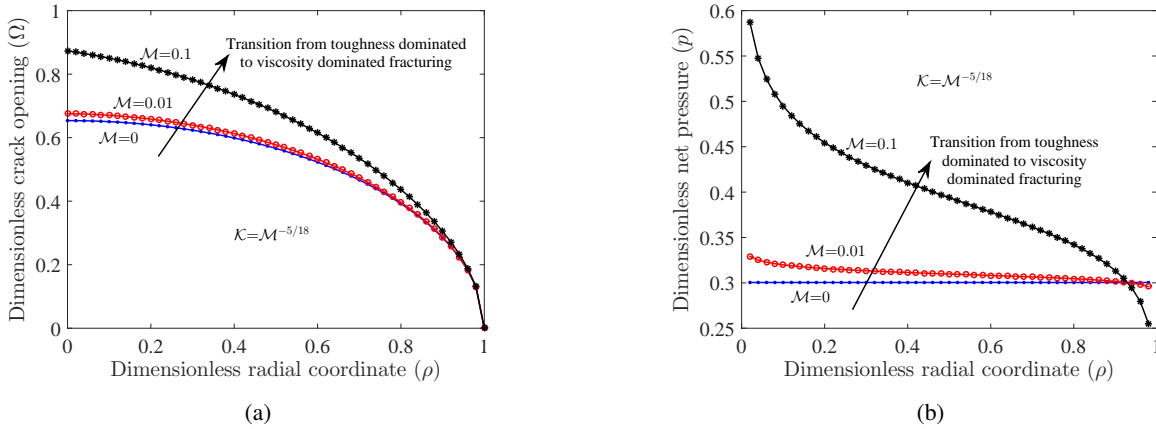


Figure 4: Dimensionless a) crack aperture profile, b) crack net pressure profile for the analytical solution of eq. (8.20) and for different values of the dimensionless viscosity  $\mathcal{M}$ .

### 8.3.3 Parametric studies

For the rock properties and operating conditions described in Johnson et al. (2013); elastic modulus  $E = 30$  MPa, Poisson’s ration  $\nu = 0.25$ , fluid dynamic viscosity  $\mu = 0.001$  Pa.s, injection rate  $Q_0 = 0.04$  m<sup>3</sup>/s, and material toughness  $K_{Ic} = 0.75$  or  $5.77$  MPa/m<sup>0.5</sup>, the time course of the dimensionless toughness,  $\mathcal{K}$ , and dimensionless viscosity  $\mathcal{M}$  can be plotted (Fig. 3).

The aforementioned analytical analysis indicates that, for the two limit cases  $\mathcal{K} = 0$  and  $\mathcal{K} \rightarrow \infty$  ( $\mathcal{M} = 0$ ), the solution is self-similar and thus does not depend on initial conditions. For any other value of  $\mathcal{K}$ , the solution is not self-similar and is a function of  $\mathcal{K}$ . In fact, since  $\mathcal{K}$  is a monotonically increasing function of time, the solution necessarily evolves from the

viscosity-dominated regime ( $\mathcal{K} \ll 0$ ) towards the toughness-dominated regime ( $\mathcal{K} \gg 1$ ), see (Fig. 4). If  $\mathcal{K}$  is the controlling parameter, the zero-toughness solution ( $\mathcal{K} = 0$ ) provides the initial conditions from which the solution will evolve.

The fracture radius in a viscosity scaling,  $\gamma_m$ , can be obtained as a function of the dimensionless toughness if the analytical solution is derived in a viscosity scaling regime, Savitski and Detournay (2002),

$$\gamma_m = \gamma_0 \mathcal{K}^{-2/5} + \gamma_1 \mathcal{K}^{-4}, \quad \text{for } \mathcal{K} \geq 1. \quad (8.24)$$

### 8.3.4 Regimes of fracture propagation

The solution for a penny-shaped hydraulic fracture depends only on one parameter, which is selected to be the toughness  $\mathcal{K}$ . In principle, three regimes of propagation can be defined:

- viscosity-dominated regime ( $\mathcal{K} < \mathcal{K}_m$ ), where the solution can be approximated by the zero-toughness solution;
- mixed-regime ( $\mathcal{K}_m < \mathcal{K} < \mathcal{K}_k$ ), where the solution depends on both the viscosity and the toughness;
- toughness-dominated regime ( $\mathcal{K} > \mathcal{K}_k$ ), where the solution can be approximated by the zero-viscosity solution).

Strictly speaking, the viscosity- and toughness-dominated regimes of propagation correspond to  $\mathcal{K} \ll 1$  and  $\mathcal{K} \gg 1$ , respectively. It is possible, however, to identify the bounds  $\mathcal{K}_m$  and  $\mathcal{K}_k$ , such that  $\mathcal{K} < \mathcal{K}_m$  corresponds for all practical purposes to the viscosity-dominated regime, and  $\mathcal{K} > \mathcal{K}_k$  to the toughness-dominated regime. Pragmatically, these bounds can be assessed by considering the dependence of the fracture radius  $\gamma_m$  on  $\mathcal{K}$ , with  $\gamma_m$  being the dimensionless fracture radius in the viscosity scaling, eq. (8.24).

The boundaries of the regimes of propagation are best determined from (Fig. 5) showing the dependence of the fracture radius in the viscosity scaling,  $\gamma_m$ , on the toughness  $\mathcal{K}$ . The numerical results suggest that  $\mathcal{K}_m \approx 1$  and  $\mathcal{K}_k \approx 3.5$  (which is consistent with the estimate based on comparing the zero- and the first-order solution for large toughness). The transition regime appears to correspond to a remarkably small interval of  $\mathcal{K}$ .

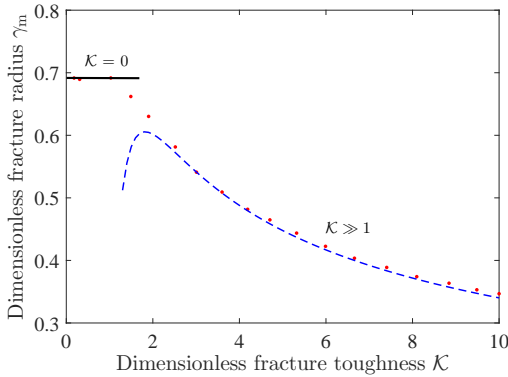


Figure 5: Dependence of the dimensionless fracture radius in the viscosity scaling  $\gamma_m$  on the dimensionless toughness  $\mathcal{K}$ . The dots correspond to the zero-order solutions and the dashed line corresponds to the first-order solution, concluded from Savitski and Detournay (2002).

The curve  $\gamma_m(\mathcal{K})$ , plotted in (Fig. 5), is in principle travelled from left to right with increasing time. Although this result could be interpreted to mean that a radial fracture starts in the viscosity-dominated regime, it should be reminded that none of the solutions discussed in Savitski and Detournay (2002) are applicable to the “early time” of fracture initiation. Indeed, the well radius has been assumed negligible compared to the fracture dimension. In fact, a radial fracture starts its existence in the toughness-dominated regime, matures in the viscosity-

dominated regime, and ages back in the toughness-dominated regime.

The regime of fracture propagation, whether toughness or viscosity dominated, needs to be determined a priori based on the initial operating conditions and rock properties by calculating the time course of  $\mathcal{K}$ , as in (Fig. 3). The question is of fundamental importance for numerical modeling. If toughness is relevant, the shape of the fracture must be determined by tracking the fracture tip, i.e. a fracturing criterion is need. If not, the fracture shape can be identified by the fluid front, which is much easier to follow than the fracture edge.

Table 1: The typical values of the parameters to control the mechanism of fracture propagation, Savitski and Detournay (2002).

Quantity	Range (Min–Max)	Unit
Injection rate, $Q_0$	0.03–0.08	$\text{m}^2/\text{s}$
Elastic modulus, $E$	7–40	GPa
Poisson’s ratio, $\nu$	0.15–0.4	-
Dynamic fluid viscosity, $\mu$	0.1–0.5	Pa.s
Fracture toughness, $K_{Ic}$	0.5–2	$\text{MPa}\sqrt{\text{m}}$

It is of interest to estimate the times at which transitions between regimes of propagation occur, given realistic values of the parameters defining  $\mathcal{K}$ . Consider Table (1) listing typical ranges of values of those parameters. According to this table, the fracture would remain in the viscosity-dominated regime for many years if all the parameters assume average values. Although the viscosity-dominated regime would be over if all the parameters are set to extreme values in favor of toughness, it would still take several years before the toughness-dominated regime is reached, see (Fig. 6). This analysis shows that radial hydraulic fractures in impermeable rocks generally propagate in the viscosity regime, and that the toughness regime is relevant only in exceptional circumstances. This observation has profound consequences for the implementation of a propagation criterion in numerical simulators of hydraulic fractures.

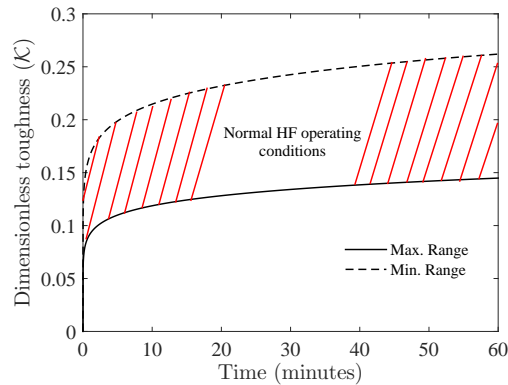


Figure 6: The development of the dimensionless toughness over a typical HF stimulation test of one hour for the rock properties and operating conditions defined in Table (1).

## 8.4 Examples: GEOS verification

The GEOS approach has been verified against the analytical solution for the viscosity and toughness dominated regimes for radial fracture propagation, Sect. (8.3). The GEOS has been also verified for the viscosity dominated regime for lateral fracture propagation. The ability of fractures to influence each other, which is one of several natural advantages of using such an approach, is confirmed by an example of competing parallel fractures, Settgest et al. (2004).

Besides hydraulic fracture stimulation and flow through fracture networks, the GEOS framework has also been applied to:

- detailed Hydro–Chemo–Mechanical (HCM) simulations of reactive flow and transport of CO<sub>2</sub> through fractures, and;
- evaluation of short– and long–term seismicity changes due to pore pressure perturbations along the fault (i.e., risk assessment for induced seismicity).

## 8.5 The GEOS simulation framework: Requirements

The previously described numerical approaches to explicitly capturing both fine and coarse scale fracture initiation and propagation as well as the effective continuum method for capturing the same at sub–REV scales must be implemented within a numerical framework if the developments are to be applicable to problems of practical interest.

This framework, at a minimum, must include the appropriate facilities for:

- large–scale (i.e., high performance computing) calculation and communication;
- appropriate solvers for the numerical approaches;
- facilities to provide dynamic topological changes in parallel for unstructured meshes;
- data structures optimized for the communication and calculation requirements;
- appropriate material modeling framework with the ability for users to easily add new models, and;
- massively parallel input and output.

As part of a multi–year effort to address energy security issues in the geosciences, LLNL has funded the Computational Geosciences group to design and implement the GEOS framework, which satisfies these requirements. Specifically, GEOS provides a general HPC simulation platform for Lagrangian computational geosciences applications with linear scaling at job sizes greater than 32 processes.

Currently, a number of numerical techniques that leverage the massively parallel code infrastructure have been implemented within the GEOS framework, including finite element, finite volume, discrete element, and boundary element methods. Both implicit and explicit solvers are available, including a fully–coupled, implicit solver for hydro–mechanical problems with mesh topology changes. Though it is built to be a versatile platform, the specific focus of GEOS development is targeted at better characterizing reservoir response to fluid–induced perturbations, including different stimulation and fracture control techniques and enhanced geothermal systems (EGS).

## 8.6 Conclusion

A fully coupled Finite Element/Finite Volume approach to modeling the evolution of hydraulic fractures using the GEOS code framework is presented. The capabilities of the GEOS code to account for multiple fluid–driven fractures evolution, as well as interaction with pre–existing heterogeneities through multi–scale treatment is discussed. The analysis of the propagation of a penny–shaped hydraulic fracture in an impermeable elastic rock is reproduced from the work of Savitski and Detournay (2002). The analytical solution of the penny–shaped hydraulic fracture has proven that radial hydraulic fractures in impermeable rocks generally propagate in the viscosity regime, and that the toughness regime is relevant only in exceptional circumstances.

## 8.7 Acknowledgments

The authors would like to thank the sponsors of the Microseismic Industry Consortium and NSERC for their financial support. The authors feel indebted to the original developers/source of the respective codes (Y-Geo and GEOS); specifically thanking Giovanni Grasselli and Scott Johnson for their assistance in implementing them.

## 8.8 References

- Savitski, A. and Detournay, E., 2002, Propagation of a penny–shaped fluid–driven fracture in an impermeable rock: Asymptotic solutions: *International Journal of Solids and Structures*, **39**, 6311–6337.
- Johnson, S., Arson, C., and Settgest, R., 23–26 June 2013, Multi–scale fracture creation and network generation during fracturing: In *Proceedings of the 47<sup>th</sup> US Rock Mechanics/Geomechanics Symposium Held in San Francisco, CA, USA*.
- Settgest, R., Johnson, S., Fu, P., and Walsh, S., 25–27 August 2014, Simulation of hydraulic fracture networks in three dimensions utilizing massively parallel computing resources: In *Proceedings of the Unconventional Resources Technology Conference Held in Denver, Colorado, USA*.

Lamb, H., 1945, Hydrodynamics: Sixth ed. Dover Publications,  
New York, NY, USA, 738 pp.  
Atkinson, B., K., 1991, Fracture mechanics of rocks: Academic

Press Limited, London, Great Britain, second printing edi-  
tion.